SAND79-2196
Unlimited Release
UC-37

Neutron Activation System for Spectral Measurements of Pulsed Ion Diode Neutron Production

David L. Hanson, Lyle W. Kruse

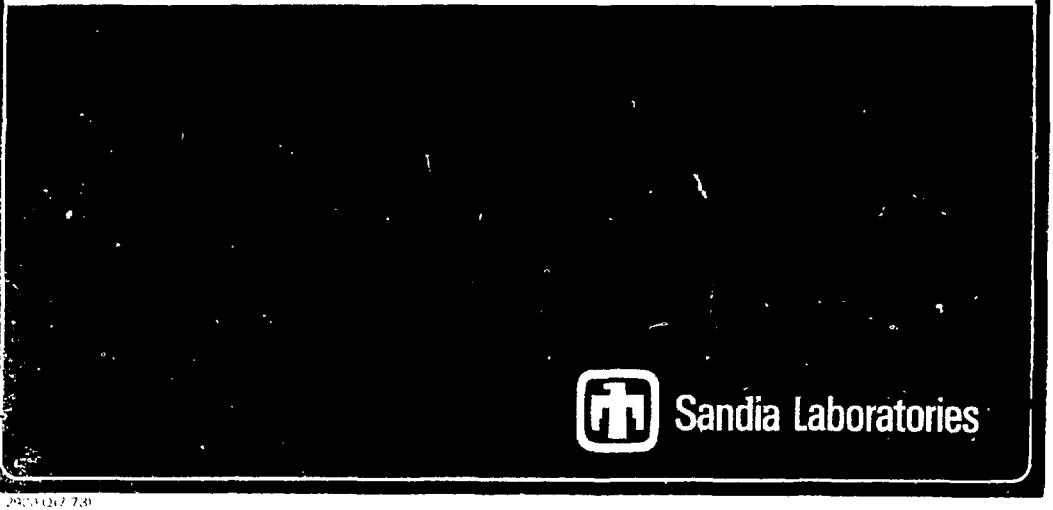

Sandia Laboratories

I. Introduction

The ability to characterize neutron energy spectra is essential for the application of intense pulsed neutron sources to radiation effects simulation and fusion materials damage studies. However, the problems of neutron detection are particularly severe in the environment of relativistic electron beam (REB) accelerators where intense electromagnetic and bremsstrahlung x-ray pulses are generated. A system for detecting neutrons in such a harsh radiation environment has been developed for use with Sandia's pulsed accelerators and is described in a previous report.[1] The essential components of this system are:

(1) total neutron yield detectors (Ag activation counters)[2] to determine the total number of neutrons from a pulse;

(2) a fast response time, high efficiency time-of-flight (TOF) spectrometer, consisting of a shielded liquid scintillator and gated photomultiplier of special design, to characterize the time distribution and approximate energy spectrum of the neutrons; and

(3) a neutron activation system to accurately determine the neutron energy spectrum.

This integrated diagnostic system is able to provide a complete picture of the time and energy distribution of neutrons produced in a REB diode shot. However, the neutron activation system of Ref. 1 made use a NaI(Tl) well crystal

to detect residual activity and was severely limited in its effectiveness by coincidence sum effects. The purpose of the present report is to describe the design of a much improved neutron activation system and its application as a neutron spectrometer in a recent series of Hermes II neutron production experiments.

This newly developed neutron activation system exploits the high resolution and high efficiency of two multiplexed Ge(Li) detectors, together with an annihilation gamma coincidence system, to measure the induced activities of a large number of irradiated samples. Samples of very short half-life are quickly returned to the counting station by a pneumatic transport system. Specific activities for the samples are determined by computer analysis of the Ge(Li) gamma spectra. The differential neutron yield as a function of energy is finally determined from the measured specific activities using an integral spectrum unfolding code together with additional constraints provided by total neutron yield and TOF measurements.

In Section II, the activation system hardware will be described in more detail, while Section III will discuss the samples and techniques employed in the activation measurements. Section IV will describe the application of the total neutron detection system to neutron spectral measurements in a recent series of experiments in which Hermes II was operated in the reverse polarity ion beam mode as an intense pulsed neutron source.

II. Description of Neutron Activation System

The arrangement of the complete neutron diagnostic system as deployed in the Hermes II experiments is shown in Fig. 1. Total neutron yield detectors were positioned at 0° and 90° to measure the asymmetry in neutron production. Two TOF detectors were located along the 0° axis and observe essentially the same neutron spectrum seen by the activation samples located on the beam axis directly behind the Hermes II faceplate.

The neutron activation system consists of a Flex-o-Rabbit[3] pneumatic system for rapidly transporting samples of short half-life from the irradiation point to the counting station, two high efficiency Ge(Li) detectors for measuring residual gamma activities from irradiated samples, and an annihilation gamma coincidence system for determining specific activities of samples which decay by positron emission.

Each Ortec[4] TEC-20 coaxial Ge(Li) detector has an efficiency of approximately 20% of that of a 3 x 3 inch diam. NaI(Tl) crystal for detecting 1.33 MeV gammas at 25 cm. The excellent energy resolution (2.1 keV at 1.33 MeV) and peak-to-Compton ratio (46:1) of these detectors make possible the use of a large number of nuclides in an activation sample and computer analysis of the resulting gamma spectra. The two detectors are multiplexed in a face-to-face geometry using an Ortec 475 Matching Multiplexer which sums the efficiencies and averages the energy resolution and peak-to-Compton ratios of the detectors. Amplified signals from the Ge(Li) system are pulse height analyzed in an Ortec 6420 4096-channel multi-

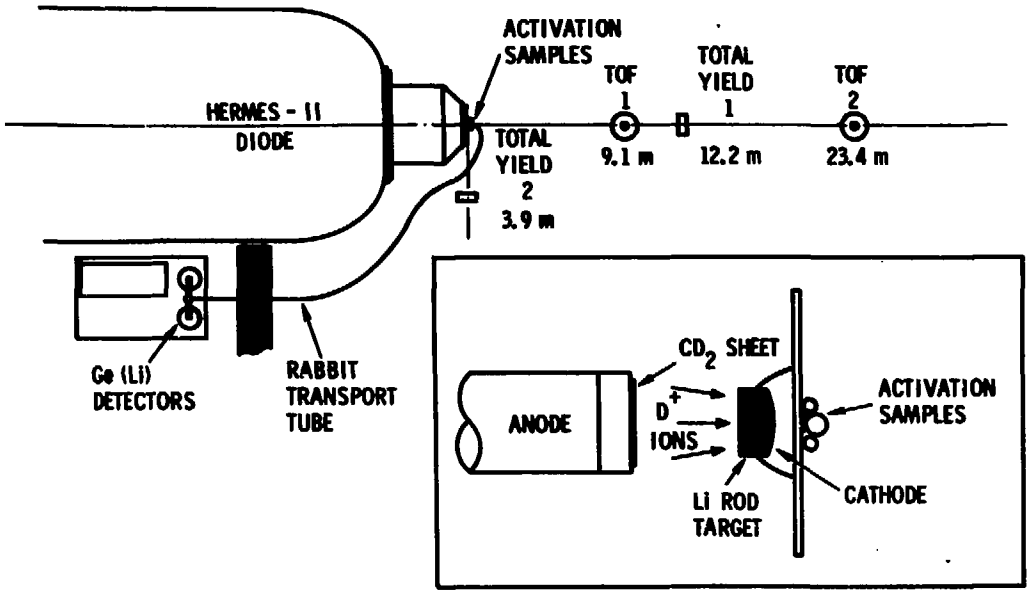

FIG. 1. GEOMETRY OF NEUTRON DETECTION SYSTEM. INSET SHOWS HERMES II DIODE CONFIGURATION FOR A TYPICAL SHOT WITH A DEUTERON SOURCE AND LITHIUM TARGET.

channel analyzer (MCA) and the resulting spectra are then transferred over an interactive link to the Sandia NOS CDC6600 Time-share Computing System for analysis.

Before each series of activation measurements, an absolute efficiency and energy calibration of the Ge(Li) detector system is carried out. Calibrated 1μCi gamma-ray sources consisting of ^{133}Ba, ^{137}Cs, ^{54}Mn, and ^{60}Co, with the gamma-ray energies listed in Table I, are counted in the standard geometry. The calibration spectrum is then transferred from the MCA to the NOS system for analysis using the program CALDAT (Appendix I). Quadratic energy calibration coefficients and efficiencies are outputs from this program.

A gamma-gamma coincidence system is used to measure residual activity of nuclides which decay by positron emission. The two 0.511 MeV gammas emitted at 180° following positron annihilation are detected by two 3 x 3 inch NaI(Tl) crystals positioned in face-to-face geometry around a flat sample. A discriminator window is set around each 0.511 MeV photopeak and signals within the correct energy range from each detector are fed to a fast coincidence unit. Coincidence events then are counted in appropriate intervals to determine the activity and decay half-life of the sample. Typical background coincidence rates of 4 counts/min. are observed for this system operated in a screen room.

III. Neutron Activation Measurement Techniques

Neutron activation analysis has a long history[5] and has

TABLE I. CALIBRATION SOURCES

Source	Gamma Energy (keV)
^{133}Ba	276.
	302.
	356.
	382.
^{137}Cs	661.6
^{54}Mn	835.3
^{60}Co	1173.
	1332.5
$[^{88}Y]^{\dagger}$	898.2
	1836.2

---

†In future work, a ^{88}Y calibration source will be used together with the other sources to span the entire range of activation sample gamma energies.

become the standard method[6] for measuring low resolution or "smoothed" neutron spectra. In this method, a sample in a neutron flux is activated through the conversion of stable isotopes to radioactive products by neutron induced nuclear reactions. Following irradiation, the induced activity is measured. This technique is particularly appropriate for use with intense pulsed neutron sources where pulse height analysis for individual neutrons is impossible and where accelerator noise would otherwise be a problem.

The specific activity A_i of a radioactive nuclide i is related to the differential spectrum $\phi(E)$ of the incident neutron beam through the integral equation

$$A_i = \int_0^\infty \sigma_i(E)\ \phi(E)dE \qquad (1)$$

where:

$\sigma_i(E)$ = differential reaction cross section for production of the ith nuclide.

In principle, the neutron energy spectrum can be deduced from activation measurements involving a sufficient number of reactions with different energy-dependent cross sections.

The activation system, by detecting gammas, betas, or positron annihilation radiation, measures the number of disintegrations $D_i(\Delta t)$ of the radioactive nuclide i in a time interval Δt. The specific activity A_i of the sample is then related to the measured $D_i(\Delta t)$ by:

$$A_i = \frac{D_i(\Delta t)}{N_i(1-e^{-\lambda_i \Delta t})e^{-\lambda_i t_c}} \qquad (2)$$

where:

N_i = number of target nuclei in the sample which may be transformed by the reaction into nuclide i;

$\lambda_i = \frac{\ln 2}{T_{\frac{1}{2}}}$ = decay constant for the activated nuclide i;

t_c = delay time between the end of the irradiation pulse and the beginning of the counting period Δt.

In the special case of most interest, where the nuclide i decays by β^- emission followed by the emission of a gamma ray of energy E_γ from the daughter nucleus, $D_i(\Delta t)$ is given in terms of the observed photopeak area P in the gamma spectrum by:

$$D_i(\Delta t) = \frac{P}{\varepsilon(E_\gamma)B} \qquad (3)$$

where:

$\varepsilon(E_\gamma)$ = absolute photopeak efficiency of the system for detecting a gamma of energy E_γ;

B = branching ratio for E_γ emission following decay of nuclide i.

It is evident from these relationships that the sensitivity of an activation measurement can be enhanced through the use of large samples having large reaction cross sections and short product half-lives, and by beginning the counting period as soon as possible after irradiation.

The isotopes used as activation samples for the present system are listed in Table II. Additional information on sample composition is presented in Appendix 2. As shown in

TABLE II. NEUTRON ACTIVATION SAMPLES

	Nuclide	Reaction	IUNFLD Foil No.	Reaction Threshold (MeV)	Product Half-life	Gamma energy (MeV)
Rabbit Sample	Al	$^{27}Al(n,p)^{27}Mg$	23	1.29	9.5m	0.842, 1.013
		$^{27}Al(n,\alpha)^{24}Na$	10	3.13	15.0h	1.369
	Na	$^{23}Na(n,p)^{23}Ne$	17	3.60	37.6s	0.439
		$^{23}Na(n,\alpha)^{20}F$	18	3.87	11.4s	1.63
	Si	$^{28}Si(n,p)^{28}Al$	15	3.86	2.31m	1.780
Independent Samples	Ni	$^{58}Ni(n,p)^{58}Co$	6	0	71.3d	0.811
	Fe	$^{56}Fe(n,p)^{56}Mn$	7	2.92	2.576h	0.847, 1.811
	Mg	$^{24}Mg(n,p)^{24}Na$	8	4.73	15.0h	1.369
Annihilation Coincidence Measurement	Cu	$^{65}Cu(n,2n)^{64}Cu$	21	9.91	12.8h	0.511
		$^{63}Cu(n,2n)^{62}Cu$	22	10.9	9.8m	0.511
Other Possible Samples	S	$^{32}S(n,p)^{32}P$	4	0.93	14.3d	β^-
	O	$^{16}O(n,p)^{16}N$	16	9.64	7.2s	6.131

Fig. 2, the neutron activation cross sections for these samples have thresholds ranging from 0 MeV for $^{58}Ni(n,p)^{58}Co$ to 10.9 MeV for $^{63}Cu(n,2n)^{62}Cu$ and peak activation cross sections from about 100mb to 1b.

Nuclides were chosen for the rabbit sample whose products have short half-lives (11.4 seconds for the $^{23}Na(n,\alpha)^{20}F$ reaction). The rabbit capsule is transported from the irradiation point to the counting area by the pneumatic transport system in an average of 2.2 seconds, which is more than adequate for the shortest half-lives of interest. A Ge(Li) detector spectrum (2000 sec counting time) from the rabbit activation sample for Shot 16816 is shown in Fig. 3.

Independent samples of Fe, Mg, and Ni are irradiated and counted with the Ge(Li) system following the rabbit sample analysis. Fe and Mg are not included in the rabbit sample because of overlapping photopeaks and the need for larger samples to compensate for longer half-lives.

The characterization of the lowest energy portion of the neutron spectrum presents certain problems. The nickel sample is presently used for this purpose. However, the $^{58}Ni(n,p)$ reaction produces ^{58}Co with a very long half-life of 72 days, and therefore requires a total yield of $\sim 10^{12}$ n and a counting time of 10 hours to produce useful statistics. In future work, a measurement of the β^- decay for the $^{32}S(n,p)^{32}P$ reaction with a product half-life of 14.3 days will be used to provide additional information on low energy neutrons. There are a number of other reactions such as

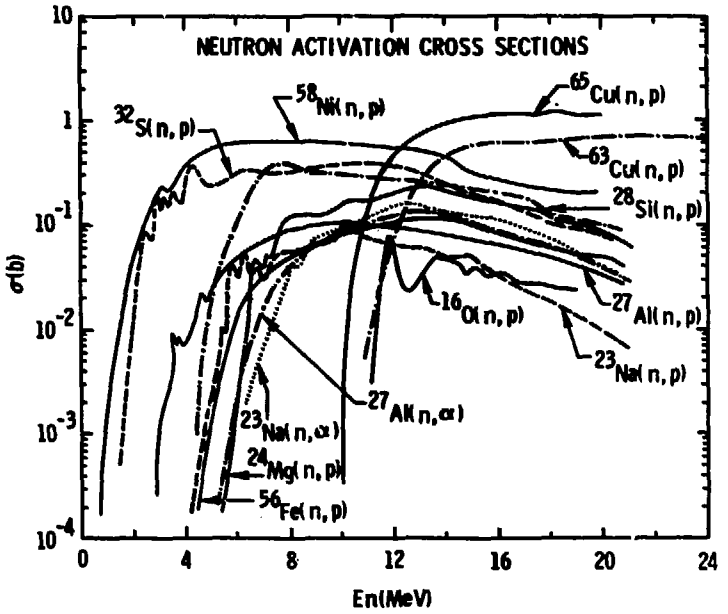

FIG. 2. NEUTRON ACTIVATION CROSS SECTIONS FOR SAMPLES USED IN PRESENT SYSTEM. CROSS SECTIONS FOR $^{32}S(N,P)^{32}P$ AND $^{16}O(N,P)^{16}N$, USEFUL REACTIONS FOR FUTURE MEASUREMENTS, ARE ALSO SHOWN.

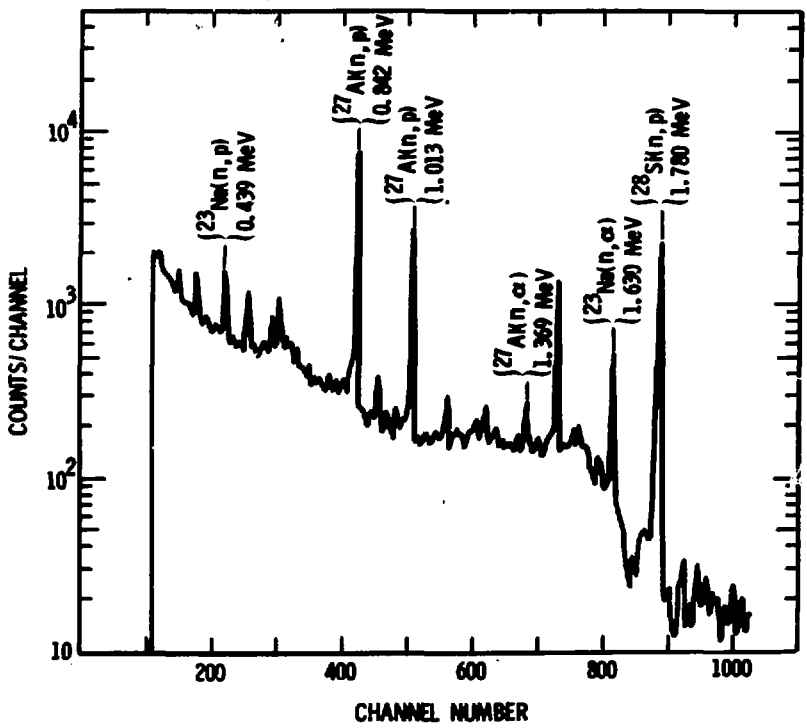

FIG. 3. GE(LI) SPECTRUM FOR RABBIT ACTIVATION SAMPLE (SHOT 16816, TOTAL NEUTRON YIELD 3.0×10^{12}N).

$^{51}V(n,p)^{51}Ti$ and $^{55}Mn(n,\alpha)^{52}V$ which have low reaction thresholds, very short half-lives, and non-interferring gamma rays, but which cannot be used to characterize the low energy part of the neutron spectrum because their reaction cross sections have been measured over only a limited energy range.

Copper samples provide a useful measure of the high energy component of the neutron spectrum. Irradiated samples decay by positron emission and the resulting annihilation radiation is detected with a NaI gamma-gamma coincidence system (see Sec. II). It would be desirable in future experiments to measure the 6.131 MeV gammas from the $^{16}O(n,p)^{16}N$ reaction (product half-life 7.2 secs) as an additional source of information on the high energy portion of the neutron spectrum. Oxygen is already present in the rabbit sample in the form of SiO_2 (Appendix 2) and the high energy gammas could be counted in an independent measurement using a NaI crystal-discriminator-scaler combination.

Neutron spectrum measurements are made with this activation system using the following procedure:

1) Prior to the shot, Fe, Ni, Mg, and Cu samples are positioned near the point of maximum neutron irradiation; the rabbit activation sample is also transferred from the screen room to the irradiation point;
2) Firing of the accelerator automatically gates on the TOF and total yield detectors, the MCA, and a timer which measures the time delay between the shot and

the return of the rabbit sample to the Ge(Li) detector counting station;

3) Immediately following the pulse, the rabbit sample is returned, the delay timer turns off, and analysis of the sample continues for a predetermined counting period;

4) The other activation samples are retrieved and analysis of the Cu sample begins with the annihilation gamma coincidence system;

5) When analysis of the rabbit sample is complete, the MCA Ge(Li) spectrum is written to cassette tape and then transferred to an NOS system file where a peak area analysis is performed using the code GELDAT (Appendix 1);

6) The other samples are analyzed with the Ge(Li) system in order of increasing product half lives; the Ni sample is counted for an extended period overnight;

7) Specific activities are determined from the activation data using the code SPAC (Appendix 1);

8) The set of 8 to 10 specific activities, together with total yield and TOF information, is input to the integral unfolding code IUNFLD which determines the neutron energy spectrum.

IV. Neutron Spectra from Activation Data Analysis

In a recent series of experiments (June 1979) the Hermes II diode was operated in the reverse polarity ion beam mode to

investigate its potential as an intense pulsed neutron source for radiation effects simulation and material damage studies. The complete neutron spectrometer was used for the first time in these experiments to characterize neutron spectral shapes. In this Section, the procedure for analyzing the neutron diagnostic data and some experimental results from these tests will be presented.

The basic arrangement of the Hermes II diode for neutron production is shown in the inset of Fig. 1. The diode is operated in reverse polarity by a reversal of the Marx generator and potential grading rings. A plasma is created during prepulse by surface flashover of a deuterated polyethylene sheet on the anode. The deuteron ions are then accelerated into a Li rod cathode during the main pulse and produce neutrons primarily by the $^{7}Li(d,n)^{8}Be$ reaction. Hemispherical carbon cathodes were also used as targets. This reverse polarity axial diode geometry has the advantage that the neutron activation samples can be located directly behind the target but outside of the diode for convenient access.

While neutron activation measurements have long been used for estimating neutron spectra, the mathematical problems of unfolding activation data to obtain differential neutron spectra have received serious attention only in the past several years. The main advance in this area has been the development of the integral spectrum unfold code IUNFLD[7] by R. E. Jones of Sandia. This interactive code is an adaptation of the program UNFOLD[8] developed by F. Biggs and D. Amos of Sandia to solve integral

equations of the first kind.

Eq. 1 (Section III) is mathematically underdetermined so specific activities alone cannot yield a solution for $\phi(E)$. IUNFLD uses activation data together with equality and inequality constraints on $\int\phi(E)dE$, $\phi(E)$, $\phi'(E)$, and $\phi''(E)$ from total yield and TOF measurements to determine the most probable neutron spectrum. A trial spectrum may be entered, but is not required for a solution. IUNFLD is unique among integral unfold codes in that it can assign a confidence level to its spectrum solution based on a mathematically rigorous weighting of all input information in proportion to its accuracy. Additional discussion of the program IUNFLD and its various applications may be found in Refs. 1 and 7.

The general interactive procedure followed to obtain an IUNFLD neutron spectrum from the Hermes total yield, TOF, and activation data is the following:

(1) A solution is found based on the total yield, specific activities, and a minimum of other constraints; this solution will in general be highly oscillatory but should have the general characteristics of the TOF spectrum;

(2) Additional equality and inequality constraints taken from the TOF spectrum are gradually imposed in successive iterations until sharp osciallations are removed and the IUNFLD solution reflects the qualitative features of the TOF spectrum;

(3) Constraints are further modified until the measured

specific activites and the calculated specific activities based on the IUNFLD solution are in optimum agreement.

As an example of the analysis required to obtain a neutron energy spectrum from diagnostic data, we will consider Hermes Shot 16817. In this shot, deuterons from a deuterated polyethylene (CD_2) anode were accelerated into a Li rod cathode and produced neutrons primarily by the $^7Li(d,n)^8Be$ reaction.

The total neutron yield, based on an average of the 0^o(12.2m) and 90^o(3.9m) Ag activation counters, was 1.0×10^{12} n on this shot. For these high yields, the Ag counter geometry was chosen such that the maximum count rate in a one minute interval was $< 5 \times 10^4$ for the 0^o detector and $< 3 \times 10^5$ for the 90^o detector, and meaningful dead time corrections could be made.[2] Another consideration in the use of Ag counters for total yield measurements is that their sensitivity as a function of neutron energy varies by about a factor of two between E_n = 2.4 and 14 MeV. The average of calibration factors at these two energies was used to determine total yield. Relative yields for the two detectors were consistent with the expected asymmetry of the $^7Li(d,n)^8Be$ reaction on a thick target.

The TOF spectrum for Shot 16817 and the TOF differential yield, corrected for scintillator neutron detection efficiency, are shown in Fig. 4a. Each point in the TOF spectrum represents an average over a time interval corresponding to the width of the Hermes II main pulse (80-100 ns FWHM). The effects of this averaging on the differential yield spectrum are insignificant below

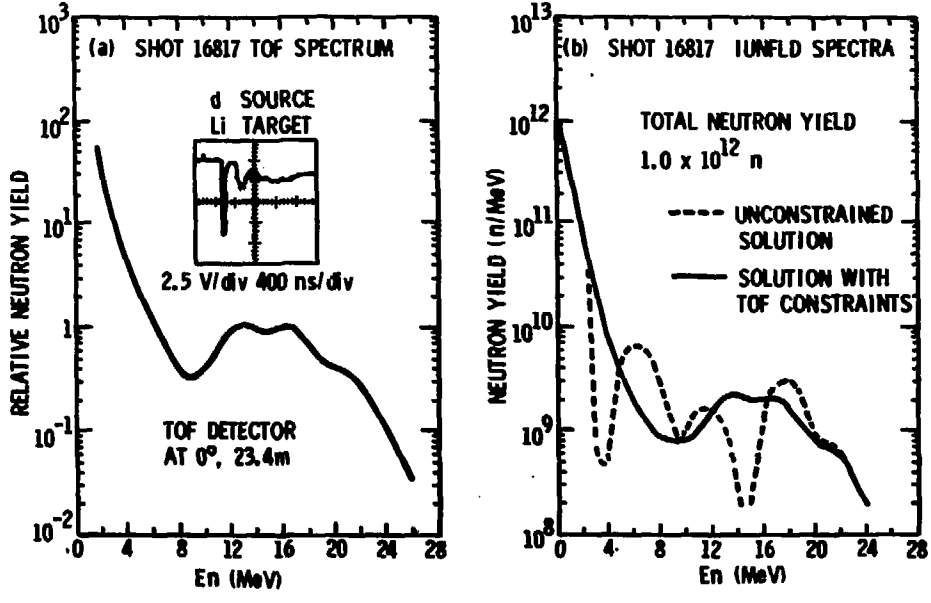

FIG. 4. A) TIME-OF-FLIGHT SPECTRUM AND TOF YIELD (CORRECTED FOR DETECTOR EFFICIENCY) FOR SHOT 16817 (D + LI); B) IUNFLD SPECTRA FOR SHOT 16817.

$E_n \sim 10$ MeV but become increasingly important as the energy averaging interval ΔE_n increases at higher neutron energies ($\Delta E_n \sim \pm 4$ MeV at $E_n = 20$ MeV). Therefore, it is a relatively low resolution TOF yield spectrum which provides constraints on the activation spectrum.

The dashed curve in Fig. 4b is a trial IUNFLD solution based on a minimum of constraints*. In addition to total yield and specific activities, the only constraints imposed on this solution were the slope and magnitude of the spectrum in the region $E_n = 21$-24 MeV (from TOF) and the requirement that the yield be greater than 0 in the region $E_n = 0$-20 MeV. This spectrum is quite oscillatory but exhibits the main qualitative features of the TOF spectrum, namely a very large low energy component and a significant component of high energy neutrons extending beyond $E_n = 20$ MeV. This spectrum is consistent with previously measured thick target yield spectra.[9,10,11] Thick target yields for the d + Li reaction at 2.0 MeV and 14.8 from Refs. 10 and 11, respectively, are shown in Fig. 5 for comparison. The direct stripping (d,n) reaction mechanism produces neutrons with an average energy $E_n \sim \frac{1}{2}E_d$ and the peak diode voltage for this shot was 8.5 MeV. Contributions from direct stripping extending up to about 4.2 MeV in the present case then could account for a significant fraction of the low energy yield. The $^7Li(d,n)^8Be$ reaction has a Q-value of +15.0 MeV.

---

*Shown here is the differential yield at 0^o normalized to the total neutron yield into 4π. The differential fluence (n/cm^2 MeV) at 0^o at the Hermes faceplate (assuming emission from a isotopic point source at 8 cm) is found by multiplying this yield by 1.24×10^{-3}.

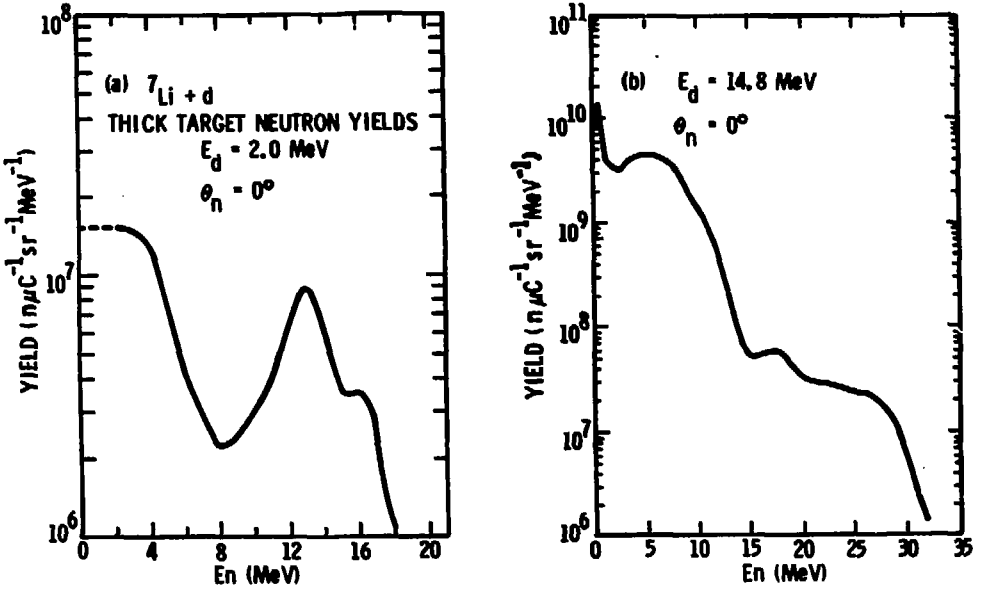

FIG. 5. THICK TARGET YIELDS FOR D + LI REACTIONS AT E_D = 2.0 MEV AND 14.8 MEV FROM REFS. 10 AND 11, RESPECTIVELY.

Thus, compound nucleus formation followed by neutron decay to the ^{8}Be ground state and excited states can produce the neutrons with energies up to E_n = 23.5 MeV which are indicated in the spectra of Fig. 4.

While the IUNFLD trial solution of Fig. 4b contains the main features of the TOF spectrum, the remaining differences in detail need to be considered. It is quite reasonable that such differences should exist. The activation samples are limited in number, and in general have low energy thresholds and smoothly varying activation cross sections above 10 MeV. Thus they provide relatively little information on the detailed shape of the spectrum at high neutron energies. By successive application of different constraints, it can be shown that a number of solutions of somewhat different shape in the region E_n >10 MeV are consistent with the available activation data. In the present case, we are forced to use the TOF spectrum shape as a guide to the most probable neutron spectrum. Constraints are imposed to produce a solution having the qualitative features of the TOF spectrum and then further modifications are introduced to bring the calculated specific activities based on the IUNFLD solution into optimum agreement with the measured specific activities. Such an IUNFLD solution based on TOF constraints is given by the solid line in Fig. 4b.

However, it is both possible and desirable to obtain an accurate high energy neutron spectrum based on neutron activation data alone, without reference to the TOF spectra.

This can be done by using additional activation samples having high activation thresholds and will be attempted in future work. Another difficulty in the present case is that only a small fraction of the total neutron yield occurs at energies above the activation threshold for most of the samples. The quality of data and accuracy of analysis would be greatly improved for a neutron spectrum more strongly weighted toward higher energies.

The general shapes of neutron spectra obtained in other shots where a CD_2 anode and a Li cathode were employed are quite similar to those of Fig. 4. The spectra for Shots 16815 and 16818 are shown in Fig. 6 as an example. The main difference between these two lies in the relative magnitudes of the high energy components of the spectra. Shot 16815 (total yield 2.7×10^{12} n) was the first with the 93 rod Li cathode. The rods at this point were covered with a residue of mineral oil (used to prevent oxidation in storage) and the high energy neutron yield from the d + Li reaction was suppressed. For Shot 16818 (total yield 1.3×10^{12} n), the last of a series of 4 shots, the Li surface was well exposed and the high energy neutron component is enhanced relative to Shot 16815.

Fig. 7 shows the TOF and IUNFLD neutron spectra for Shot 16819 where a hemispherical carbon cathode was used in place of Li rods. The peak diode voltage for this shot was 7.7 MV. However, the Q-value for the $^{12}C(d,n)^{13}N$ reaction is -0.28 MeV and the high energy component in the neutron spectrum is

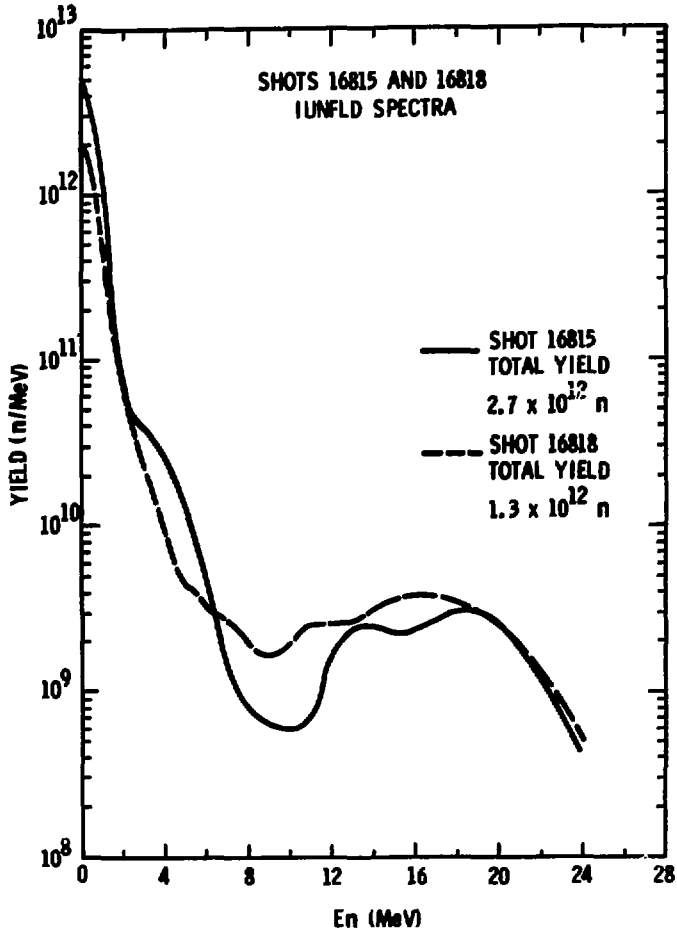

FIG. 6. IUNFLD SPECTRA FOR SHOTS 16815 AND 16818.

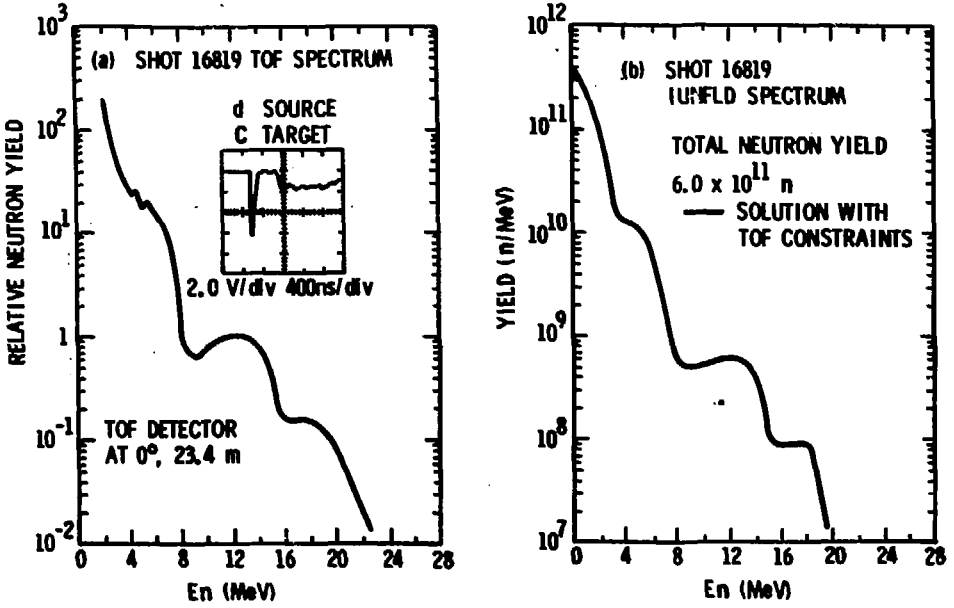

FIG. 7. A) TOF SPECTRUM AND YIELD FOR SHOT 16819 (D + C)
B) IUNFLD SPECTRUM FOR SHOT 16819.

significantly reduced.

An estimate can be made of neutron yield thresholds required to obtain a reasonably accurate neutron spectrum measurement with the present system and samples. Analysis of the Hermes data shows that a fluence of $\sim 2 \times 10^8$ n/cm^2 at 10 cm from the Li target is required to give 100 counts in the 0.439 MeV photopeak from the ^{23}Na(n,p) reaction in 2000 seconds of counting time. This is the minimum fluence required to produce a useful Rabbit sample spectrum and corresponds to a total yield of 2.3×10^{11} n. With an improved geometry where the samples are placed 4 cm from the target, this fluence could be achieved with a total neutron yield of only 3.7×10^{10} n. For a truncated system using only the ^{27}Al(n,p), ^{28}Si(n,p), and ^{63}Cu(n,2n) reactions to obtain a crude estimate of the spectrum, a minimum fluence of $\sim 4 \times 10^7$ n/cm^2 could be detected with 10% counting statistics. In the improved geometry (sample at 4 cm), this corresponds to a total yield of 8×10^9 n. It is important to note that these sensitivity estimates apply only to the d + Li neutron spectra measured in the Hermes experiments. The neutron yield in this case lies predominantly below 4 MeV, which is near or below the activation threshold for most of the samples. Were a significant fraction of the neutron yield to occur at energies $E_n > 4$ MeV, the sensitivity thresholds quoted could easily be lowered by a factor of 10^2 or more.

V. Conclusions and Future System Improvements

A neutron energy spectrometer has been developed as part of an integrated detection system for the study of neutron production in pulsed ion beam diodes. The use of high resolution Ge(Li) detectors in the threshold neutron activation system makes possible the simultaneous measurement of a large number of specific activities and accurate determination of neutron spectra over a broad energy range. Additional constraints on the neutron spectra are provided by total neutron yield and TOF measurements. The ability of this system to characterize the differential neutron fluence spectrum from a pulsed ion diode has now been demonstrated in neutron production experiments on Hermes II.

There are a number of possible improvements to this neutron activation system which would significantly increase its accuracy, sensitivity, and flexibility. These include:

(1) The addition of measurements on samples such as sulfur and oxygen which would improve the quality of information available on the low and high energy extremes of the neutron spectrum;

(2) The addition of Pb shielding around the Ge(Li) detectors to reduce background levels, improve sensitivity, and facilitate the computer analysis of gamma spectra in low neutron yield situations; and

(3) The use of additional Cu samples and gamma-gamma coincidence systems to characterize the spatial

distribution of high energy neutrons in large area ion diodes.

ACKNOWLEDGEMENTS

The authors wish to thank J. E. Harness and the Hermes II operations group (4232) as well as the personnel of the Sandia Simulation Instrumentation Division 1126 for their excellent support during the neutron production experiments on Hermes II.

REFERENCES

1. Lyle W. Kruse, "A System for Detecting Neutrons in the Harsh Radiation Environment of a Relativistic Electron Beam," Sandia Laboratories Report SAND78-0513.

2. R. J. Lanter and D. E. Bannerman, "The Silver Counter: A Detector for Bursts of Neutrons," Los Alamos Scientific Laboratory Report LA-3498-MS, July 1966.

3. Reactor Experiments Inc., 963 Terminal Way, San Carlos, CA 94070.

4. Ortec, Inc., 100 Midland Road, Oak Ridge, TN 37830.

5. B. L. Cohen, "High Energy Neutron Threshold Detectors," Nucleonics 8, No. 2, 29 (1951).

6. P. Kruger, Principles of Activation Analysis, John Wiley & Sons (1971).

7. R. E. Jones, J. M. McKenzie, and L. A. Romero, "Differential Neutron Spectrum Unfolding from Foil Activation Data," IEEE Trans. Nucl. Sci. NS-24, 2540 (1977).

8. F. Biggs and D. Amos, "Numerical Solution of Integral Equations and Curve Fitting," Sandia Laboratories Report SC-RR-71-0212, September 1971.

9. K. A. Weaver, "Neutrons from Deuteron Bombardment of Light Nuclei," UCLR-51310 and Addendum (LLL, 1973); and K. A. Weaver, J. D. Anderson, H. H. Barschall, and J. C. Davis, "Neutrons from the Bombardment of Beryllium by Deuterons," Phys. Med. Biol. 18, 64 (1973).

10. D. T. L. Jones and C. M. Bartle, "Neutrons from the 2 MeV Deuteron Bombardment of Thick ^{7}Li Targets," Nucl. Instrum. and Meth. 118, 525 (1974).

11. M. A. Lone, C. B. Bigham, J. S. Fraser, H. R. Schneider, T. K. Alexander, A. J. Ferguson, and A. B. McDonald, "Thick Target Neutron Yields and Spectral Distributions from the $^{7}Li(p,n)$, $^{7}Li(d,n)$, and $^{9}Be(p,n)$, $^{9}Be(d,n)$ Reactions," Nucl. Instrum, and Meth. 143, 331 (1977).

APPENDIX 1

```
OLD,CALDAT

READY.
LNH

00100 PROGRAM CALDAT(INPUT,OUTPUT,TAPE20,TAPE30)
00110C ENERGY AND EFFICIENCY CALIBRATION PROGRAM
00120C FOR GE(LI) DETECTOR SYSTEM
00121C
00122C CALIBRATION STANDARD CONSISTS OF MN54, CO60, BA133, AND CS137
00123C CALIBRATION SOURCES IN RABBIT SAMPLE GEOMETRY
00124C
00125C EG(I) = ENERGY (KEV) FOR GAMMA(I)
00126C EGBIG(I) = RELATIVE ENERGY RESOLUTION FOR GAMMA(I)
00127C AC(I) = CALIBRATION SOURCE ACTIVITY FOR GAMMA(I)ON 11/28/78
00128C          (GAMMAS/SEC INTO 4PI)
00129C HL(I) = HALF-LIFE (DAYS) OF GAMMA(I) CALIBRATION SOURCE
00130C
00131 DOUBLE PRECISION A,AI
00140 DIMENSION Y(4096),Y1(4096)
00150 DIMENSION EG(12),EGBIG(12),PK(12),AC(12),HL(12),SUM(12),V(12)
00160 DIMENSION A(3,3),AI(3,3),B(3),C(3),COER(3),P(3,12),EFF(12)
00170 DATA (EG(I),I=1,8)/274.,303.,356.,384.,662.,
00180+ 835.,1173.,1332./
00190 DATA (EGBIG(I),I=1,8)/1.32,1.36,1.40,1.42,1.62,1.71,1.89,1.96/
00200 DATA (AC(I),I=1,8)/2.728E+03,6.973E+03,2.332E+04,3.311E+03,
00210+ 3.554E+04,4.143E+04,4.066E+04,4.070E+04/
00220 DATA (HL(I),I=1,8)/3833.,3833.,3833.,3833.,
00230+ 10950.,312.5,1924.,1924./
00240 PRINT #,'    '
00250 PRINT #,'GE(LI) GAMMA ENERGY AND EFFICIENCY CALIBRATION'
00260 PRINT #,'DATA FILE CALBPC RETRIEVED FOR PROGRAM'
00270 CALL GETF(IERR1,20,6HCALBPC)
00280 PRINT #,'IERR1=',IERR1
00290 PRINT #,'ENTER SEARCH LEVEL'
00300 READ 5,SER
00310 5 FORMAT(F10.0)
00320 PRINT #,'SER =',SER,' = 1ST DERIVATIVE SEARCH LEVEL'
00330 PRINT #,'SUM OVER -XL,+XU CHANNELS AROUND PEAK'
00331 PRINT #,'ENTER XL'
00332 READ 5,XL
00333 PRINT #,'ENTER XU'
00334 READ 5,XU
00340 IXL=XL
00350 IXU=XU
00360 PRINT #,'ENTER LIVE TIME (SECS)'
00370 READ 5,T
00380 PRINT #,'LIVE TIME = ',T,' SECS'
00390 TMOT=33.0
00400 READ(20,25)(Y(I),I=1,4096)
00410 25 FORMAT(4X,10F7.0)
00420C SMOOTH DATA BY AVERAGING OVER 3 CHANNELS
00430 110 I=440
00440 111 I=I+1
00450 Y1(I)=(Y(I-1)+Y(I)+Y(I+1))/3.
00460 IF(I-4090)111,114,114
00470 114 PRINT #,'SPECTRUM AVERAGED'
00480 I=440
00490 115 I=I+1
00500 Y(I)=Y1(I)
00510 IF(I-4090)115,120,120
00511 120 I=440
00512 121 I=I+1
```

```
01750 WRITE 405,J,SUM(J)
01751 405 FORMAT('AREA PEAK ',I2,' = ',F10.1)
01760 410 CONTINUE
01770C DETERMINE EFFICIENCY VS. ENERGY FOR GE(LI)DETECTOR SYSTEM
01780 PRINT *,'ENTER ELAPSED TIME (DAYS) SINCE 12/31/78'
01790 READ 5,TE
01800 PRINT *,'EGAMMA (KEV)              EFF'
01810 DO 430 I=1,KK
01820 TTE=TE+TNOT
01830C ACNOW = NO. GAMMAS I EMITTED INTO 4PI IN T SECS AT TIME OF MEASUREMENT
01840 ACNOW=AC(I)*T*EXP((-0.693*TTE)/HL(I))
01850 EFF(I)=SUM(I)/ACNOW
01860 WRITE 425,EG(I),EFF(I)
01861 425 FORMAT(2X,F7.1,10X,1PE12.5)
01870 430 CONTINUE
01880 WRITE(30,435) ((EG(I),EFF(I)),I=1,8)
01890 435 FORMAT(2E14.5)
01900 REWIND 30
01910 CALL REPLACE(IERR3,30,5HPARAM)
01920 PRINT *,'IERR3=',IERR3
01930 GO TO 595
01940 570 PRINT *,'SEARCH LEVEL BELOW MIN - STOP'
01950 GO TO 595
01960 580 PRINT *,'SEARCH LEVEL ABOVE MAX - STOP'
01970 GO TO 595
01980 590 PRINT *,'DETERMINANT=0.0 - STOP'
02070 595 CALL RETURNF(20)
02080 CALL RETURNF(30)
02090 END
READY.
```

```
01120 D3=A(1,3)*(A(2,1)*A(3,2)-A(2,2)*A(3,1))
01130 DET=D1+D2+D3
01140 IF (DET.EQ.0.0) GO TO 590
01150 AI(1,1)=(A(2,2)*A(3,3)-A(2,3)*A(3,2))/DET
01160 AI(1,2)=-(A(1,2)*A(3,3)-A(1,3)*A(3,2))/DET
01170 AI(1,3)=(A(1,2)*A(2,3)-A(1,3)*A(2,2))/DET
01180 AI(2,1)=-(A(2,1)*A(3,3)-A(2,3)*A(3,1))/DET
01190 AI(2,2)=(A(1,1)*A(3,3)-A(1,3)*A(3,1))/DET
01200 AI(2,3)=-(A(1,1)*A(2,3)-A(1,3)*A(2,1))/DET
01210 AI(3,1)=(A(2,1)*A(3,2)-A(2,2)*A(3,1))/DET
01220 AI(3,2)=-(A(1,1)*A(3,2)-A(1,2)*A(3,1))/DET
01230 AI(3,3)=(A(1,1)*A(2,2)-A(1,2)*A(2,1))/DET
01240 DO 340 I=1,3
01250 DO 340 J=1,3
01260 A(I,J)=AI(I,J)
01270 340 CONTINUE
01280C COMPUTE POLYNOMIAL COEFFICIENTS C(K)
01290 DO 350 K=1,3
01300 C(K)=0.0
01310 DO 355 J=1,3
01320 355 C(K)=C(K)+B(J)*A(J,K)
01330C COMPUTE COEFFICIENT ERROR
01340 AKK=DABS(A(K,K))
01350 COER(K)=SQRT(AKK)
01360 350 CONTINUE
01370C COMPUTE CHI-SQUARED
01380 CHISQ=0.0
01390 DO 360 I=1,KK
01400 V(I)=0.0
01410 DO 365 K=1,3
01420 V(I)=V(I)+C(K)*P(K,I)
01430 365 CONTINUE
01440 Q=EQ(I)-V(I)
01450 CHISQ=CHISQ+(Q**2)/(EQSIG(I)**2)
01460 360 CONTINUE
01470C PRINT OUT CALIBRATION COEFFICIENTS
01480 PRINT *,'   '
01490 PRINT *,'E(KEV) = C(1) + C(2)*CHAN + C(3)*CHAN**2'
01500 WRITE 367,C(1),COER(1)
01501 367 FORMAT('C(1) = ',1PE12.5,5X,'COER(1) = ',1PE12.5)
01510 WRITE 368,C(2),COER(2)
01511 368 FORMAT('C(2) = ',1PE12.5,5X,'COER(2) = ',1PE12.5)
01520 WRITE 369,C(3),COER(3)
01521 369 FORMAT('C(3) = ',1PE12.5,5X,'COER(3) = ',1PE12.5)
01530 PRINT *,'   '
01540 PRINT *,'CHISQ = ', CHISQ
01550 PRINT *,'   '
01560 CALL GETF(IERR2,30,5HPARAM)
01570 PRINT *,'IERR2=',IERR2
01580 WRITE(30,370) (C(I),I=1,3)
01590 370 FORMAT(3E14.5)
01600C FIND PEAK AREAS
01610 DO 410 J=1,KK
01620 I=PK(J)
01630 TSUM=0.0
01640 IL=I-IXL
01650 IU=I+IXU
01660 DO 415 II=IL,IU
01670 TSUM=TSUM+Y(II)
01680 415 CONTINUE
01690 YA1=(Y(IL-2)+Y(IL-1)+Y(IL)+Y(IL+1)+Y(IL+2))/5.
01700 YA2=(Y(IU-2)+Y(IU-1)+Y(IU)+Y(IU+1)+Y(IU+2))/5.
01710 TCH=IXL+IXU+1
01720 BKGSUM=TCH*((YA1+YA2)/2.0)
01730 SUM(J)=TSUM-BKGSUM
01740 PRINT *,'   '
```

```
01750 WRITE 405,J,BUM(J)
01751 405 FORMAT('AREA PEAK ',I2,' = ',F10.1)
01760 410 CONTINUE
01770C DETERMINE EFFICIENCY VS. ENERGY FOR GE(LI)DETECTOR SYSTEM
01780 PRINT *,'ENTER ELAPSED TIME (DAYS) SINCE 12/31/78'
01790 READ 5,TE
01800 PRINT *,'EGAMMA (KEV)              EFF'
01810 DO 430 I=1,KK
01820 TTE=TE+TNOT
01830C ACNOW = NO. GAMMAS I EMITTED INTO 4PI IN T SECS AT TIME OF MEASUREMENT
01840 ACNOW=AC(I)*T*EXP((-0.693*TTE)/HL(I))
01850 EFF(I)=BUM(I)/ACNOW
01860 WRITE 425,EG(I),EFF(I)
01861 425 FORMAT(2X,F7.1,10X,1PE12.5)
01870 430 CONTINUE
01880 WRITE(30,435) ((EG(I),EFF(I)),I=1,8)
01890 435 FORMAT(2E14.5)
01900 REWIND 30
01910 CALL REPLACE(IERR3,30,5HPARAM)
01920 PRINT *,'IERR3=',IERR3
01930 GO TO 595
01940 570 PRINT *,'SEARCH LEVEL BELOW MIN - STOP'
01950 GO TO 595
01960 580 PRINT *,'SEARCH LEVEL ABOVE MAX - STOP'
01970 GO TO 595
01980 590 PRINT *,'DETERMINANT=0.0 - STOP'
02070 595 CALL RETURNF(20)
02080 CALL RETURNF(30)
02090 END
READY.
```

```
OLD,DELDAT

READY.
LNH.

00100 PROGRAM DELDAT(INPUT,OUTPUT,TAPE20,TAPE30)
00110C PEAK LOCATION PROGRAM FOR RABBIT SAMPLE
00120 DIMENSION Y(4096),Y1(4096),EP(90),PK(90),SUM(90)
00130 DIMENSION C(3),SUM(90),EG(12),EFF(12)
00140 DIMENSION EGS(20),FNS(20)
00150C
00160C EGS(I)=ENERGY(KEV) FOR GAMMA(I)
00170C FNS(I)=NO. IUNFLD TARGET FOIL FOR GAMMA(I)
00180C
00190 DATA (EGS(I),I=1,6)/439.0,842.0,1013.0,1369.0,
00200+ 1630.0,1780.0/
00210 DATA (FNS(I),I=1,6)/17.,23.,23.,10.,18.,15./
00220 CALL GETF(IERR1,20,5HPARAM)
00230 PRINT 8,'IERR1=',IERR1
00240 READ(20,3) (C(I),I=1,3)
00250 3 FORMAT(3E14.5)
00260 READ(20,4)((EG(I),EFF(I)),I=1,6)
00270 4 FORMAT(2E14.5)
00280 PRINT 8,'BE(LI) GAMMA SPECTRUM ANALYSIS FOR RABBIT SAMPLE'
00290 PRINT 8,'  '
00300 PRINT 8,'RETRIEVE DATA FILE DELSPC FOR PROGRAM'
00310 CALL GETF(IERR2,20,6HDELSPC)
00320 PRINT 8,'IERR2=', IERR2
00330 PRINT 8,'ENTER SEARCH LEVEL'
00340 READ 5,SER
00350 5 FORMAT(F10.0)
00360 PRINT 8,'SER = ',SER,' = 1ST DERIVATIVE SEARCH LEVEL'
00370 L=6
00380 PRINT 8,'SUM OVER -XL,+XU CHANNELS ARDUND PEAK'
00390 PRINT 8,'ENTER XL'
00400 READ 5,XL
00410 PRINT 8,'ENTER XU'
00420 READ 5,XU
00430 READ(20,23)(Y(I),I=1,4096)
00440 23 FORMAT(4X,10F7.0)
00450 60 I=440
00460 65 I=I+1
00470 Y1(I)=(Y(I-1)+Y(I)+Y(I+1))/3.
00480 IF(I-4090) 65,70,70
00490 70 PRINT 8,'SPECTRUM AVERAGED'
00500 I=440
00510 72 I=I+1
00520 Y(I)=Y1(I)
00530 IF(I-4090)72,74,74
00540 74 I=440
00550 75 I=I+1
00560 Y1(I)=(Y(I-1)+Y(I)+Y(I+1))/3.
00570 IF(I-4090)75,76,76
00580 76 PRINT 8,'SPECTRUM AVERAGED'
00590 I=440
00600 77 I=I+1
00610 Y(I)=Y1(I)
00620 IF(I-4090)77,80,80
00630 80 I=450
00640 85 I=I+1
00650 Y1(I)=(Y(I+1)-Y(I))/1.
00660 IF(I-4090) 85,90,90
```

```
00670 90 CALL GETF(IERR2,20,6HDELBPC)
00680 PRINT *,'IERR2=',IERR2
00690 READ(20,23)(Y(I),I=1,4096)
00700 100 CONTINUE
00710 PRINT *,'    '
00720 PRINT *,'    '
00730 PRINT *,'PEAK CHAN    ENERGY(KEV)      AREA      IUNFLD FOIL NO.'
00740 N=0
00750 J=0
00760 I=450
00770 120 IF(I-4090) 125,340,340
00780 125 IF(Y1(I)-BER) 150,170,170
00790 150 I=I+1
00800 GO TO 120
00810 170 IF(Y1(I)-0.) 190,190,180
00820 180 I=I+1
00830 GO TO 170
00840 190 J=J+1
00850 PK(J)=I
00860 EP(J)=C(1)+C(2)*PK(J)+C(3)*(PK(J)**2)
00870 TSUM=0.0
00880 IL=I-IXL
00890 IU=I+IXU
00900 DO 215 II=IL,IU
00910 TSUM=TSUM+Y(II)
00920 215 CONTINUE
00930 YA1=(Y(IL-2)+Y(IL-1)+Y(IL)+Y(IL+1)+Y(IL+2))/5.
00940 YA2=(Y(IU-2)+Y(IU-1)+Y(IU)+Y(IU+1)+Y(IU+2))/5.
00950 TCH=IXL+IXU+1
00960 BKGSUM=TCH*((YA1+YA2)/2.)
00970 SUM(J)=TSUM-BKGSUM
00980 MX=0
00990 DO 260 M=1,L
01000 IF((ABS(EP(J)-EGS(M))).LE.(2.*XU)) GO TO 250
01010 GO TO 260
01020 250 N=N+1
01030 MX=M
01040 260 CONTINUE
01050 IF(MX.EQ.0) WRITE 275,PK(J),EP(J),SUM(J)
01060 275 FORMAT(1X,F6.0,8X,F6.0,5X,F10.0)
01070 IF(MX.GT.0) WRITE 280,PK(J),EP(J),SUM(J),FNS(MX)
01080 280 FORMAT(1X,F6.0,8X,F6.0,5X,F10.0,9X,F3.0)
01090 GO TO 120
01100 340 KK=J
01110 PRINT *,'    '
01120 PRINT *,KK,' PEAKS HAVE BEEN IDENTIFIED'
01130 PRINT *,N,' PEAKS ASSOCIATED WITH RABBIT SAMPLE'
01140 PRINT *,'ENTER N=-1 TO DECREASE SEARCH LEVEL,'
01150 PRINT *,'   OR N=+1 TO STOP'
01160 READ 345,NN
01170 345 FORMAT(I2)
01180 IF(NN.GE.0) GO TO 570
01190 IF(NN.LT.0) GO TO 360
01200 360 SER=BER/2.
01210 IF(SER.LT.2.) GO TO 550
01220 PRINT *,'    '
01230 PRINT *,'NEW SEARCH LEVEL IS ',SER
01240 GO TO 100
01250 550 PRINT*,'1ST DERIVATIVE SEARCH PARAMETER BELOW MIN - STOP'
01260 570 CALL RETURNF(20)
01270 CALL RETURNF(30)
01280 END
READY.
```

```
OLD,SPAC

READY.
LNH

00100 PROGRAM SPAC(INPUT,OUTPUT,TAPE20,TAPE30)
00110C PROGRAM TO CALCULATE SPECIFIC ACTIVITIES FOR NEUTRON ACTIVATION SAMPLES
00120 DIMENSION EF(20),BR(20),EB(20),HL(20),AN(20),FN(20),BA(20)
00130 DIMENSION RL(20)
00140C
00150C EF(I) = GE(LI) SYS ABS EFF FOR GAMMA(I)
00160C BR(I) = BRANCH RATIO FOR GAMMA(I)
00170C EB(I) = ENERGY (KEV) FOR GAMMA(I)
00180C HL(I) = HALF-LIFE OF REACTION PRODUCT FOR GAMMA(I)
00190C AN(I) = NO. OF TARGET NUCLEI IN SAMPLE FOR GAMMA(I)
00200C FN(I) = NO. OF IUNFLD TARGET FOIL FOR GAMMA(I)
00210C BA(I) = SPECIFIC ACTIVITY FOR GAMMA(I)
00220C
00230 DATA(EF(I),I=1,12)/2.39E-02,1.26E-02,1.03E-02,
00240+ 7.61E-03,6.32E-03,5.79E-03,1.29E-02,5.62E-03,
00250+ 7.61E-03,1.32E-02,3.13E-02,3.13E-02/
00260 DATA(BR(I),I=1,12)/0.328,0.696,0.304,0.990,1.000,
00270+ 1.000,0.989,0.293,1.000,1.000,0.980,0.185/
00280 DATA(EB(I),I=1,12)/439.0,842.0,1013.0,1369.0,
00290+ 1630.0,1780.0,847.0,1811.0,1769.0,811.0,511.0,511.0/
00300 DATA(HL(I),I=1,12)/3.760E+01,5.700E+02,5.700E+02,
00310+ 5.400E+04,1.140E+01,1.324E+02,9.274E+03,9.274E+03,
00320+ 5.400E+04,6.146E+04,5.000E+02,4.608E+04/
00330 DATA(AN(I),I=1,12)/2.578E+21,1.116E+22,1.116E+22,
00340+ 1.116E+22,2.578E+21,2.310E+21,9.089E+21,9.089E+21,
00350+ 1.944E+22,1.709E+21,6.549E+21,2.929E+21/
00360 DATA(FN(I),I=1,12)/17.,23.,23.,10.,18.,15.,7.,
00370+ 7.,8.,6.,22.,21./
00380 DATA(RL(I),I=1,12)/10HNA23(N,P) ,10HAL27(N,P) ,
00390+ 10HAL27(N,P) ,10HAL27(N,A) ,10HNA23(N,A) ,10HBI2B(N,P) ,
00400+ 10HFE56(N,P) ,10HFE56(N,P) ,10HMB24(N,P) ,10HNI58(N,P) ,
00410+ 10HCU63(N,2N),10HCU65(N,2N)/
00420 10 PRINT 8,'    '
00430 PRINT 8,'    '
00440 PRINT 8,'ENTER SHOT NO.(I5)'
00450 READ 4,NS
00460 4 FORMAT(I5)
00470 PRINT 8,'ENTER NEUTRON YIELD(E7.1)'
00480 READ 6,YN
00490 6 FORMAT(E7.1)
00500 PRINT 8,'    '
00510 PRINT 8,'RABBIT SAMPLE'
00520 PRINT 8,'    '
00530 PRINT 8,'ENTER TCOR (SECS)'
00540 READ 5,TCOR
00550 5 FORMAT(F10.0)
00560 IF(TCOR.EQ.0.0) GO TO 50
00570 PRINT 8,'ENTER LIVE TIME (SECS) '
00580 READ 5,T
00590 PRINT 8,'ENTER MASS OF SAMPLE (GRAMS) '
00600 READ 5,GRAM
00610 DO 40 I=1,6
00620 ANX=AN(I)*GRAM
00630 PRINT 8,'    '
00640 WRITE 45,RL(I)
00650 45 FORMAT(1H ,10HREACTION  ,A10)
00660 PRINT 8,'EGAMMA = ',EB(I),' KEV'
```

```
00670 PRINT #,'HALF-LIFE = ',HL(I),' SECS'
00680 PRINT #,'BRANCHING RATIO = ',BR(I)
00690 PRINT #,'ENTER PEAK AREA'
00700 READ 5,SUM
00710 IF(SUM.EQ.0.0) GO TO 40
00720 SA(I)=SUM/(EF(I)*BR(I))
00730 SA(I)=SA(I)/(1.-EXP((-T*0.693)/HL(I)))
00740 SA(I)=SA(I)/EXP((-TCOR*0.693)/HL(I))
00750 SA(I)=SA(I)/ANX
00760 PRINT #,'SP. ACT. FOR IUNFLD FOIL NO. ',FN(I),' = ',SA(I)
00770 40 CONTINUE
00780 50 PRINT #,'   '
00790 PRINT #,'OTHER SAMPLES'
00800 DO 60 I=7,12
00810 PRINT #,'   '
00820 WRITE 45,RL(I)
00830 PRINT #,'EGAMMA = ',EG(I),' KEV '
00840 PRINT #,'HALF-LIFE = ',HL(I),' SECS'
00850 PRINT #,'BRANCHING RATIO = ',BR(I)
00860 PRINT #,'ENTER TCOR (SECS)'
00870 READ 5,TCOR
00880 IF(TCOR.EQ.0.0) GO TO 58
00890 PRINT #,'ENTER LIVE TIME (SECS)'
00900 READ 5,T
00910 PRINT #,'ENTER MASS OF SAMPLE (GRAMS)'
00920 READ 5,GRAM
00930 ANX=AN(I)*GRAM
00940 PRINT #,'ENTER PEAK AREA'
00950 READ 5,SUM
00960 SA(I)=SUM/(EF(I)*BR(I))
00970 SA(I)=SA(I)/(1.-EXP((-T*0.693)/HL(I)))
00980 SA(I)=SA(I)/EXP((-TCOR*0.693)/HL(I))
00990 SA(I)=SA(I)/ANX
01000 PRINT #,'SP. ACT. FOR IUNFLD FOIL NO. ',FN(I),' = ',SA(I)
01010 GO TO 60
01020 58 SA(I)=0.0
01030 60 CONTINUE
01040 PRINT #,'   '
01050 PRINT #,'   '
01060 PRINT #,'SHOT NO. ',NS
01070 PRINT #,'   '
01080 PRINT #,'TOTAL NEUTRON YIELD = ',YN
01090 PRINT #,'   '
01100 PRINT #,' REACTION    EGAMMA    IUNFLD FOIL NO.    SP. ACT.'
01110 DO 80 I=1,12
01120 WRITE 65,RL(I),EG(I),FN(I),SA(I)
01130 65 FORMAT(1X,A10,1X,F8.1,9X,F4.1,7X,1PE12.5)
01140 80 CONTINUE
01150 PRINT #,'   '
01160 PRINT #,'   '
01170 PRINT #,'   '
01180 PRINT #,'   '
01190 PRINT #,'ENTER 1 TO CONTINUE, 0 TO STOP '
01200 READ 85,NX
01210 85 FORMAT(I1)
01220 IF(NX.EQ.1) GO TO 10
01230 90 CONTINUE
01240 END
READY.
```

APPENDIX 2. NEUTRON ACTIVATION SAMPLES

Sample	Composition (by weight)	Atoms/gm Sample		Typical Sample Weight (g)	Atoms/Sample
Rabbit	2 parts Al	^{27}Al	1.12×10^{22}	20	2.2×10^{23}
	:1 part SiO_2	^{28}Si	2.31×10^{21}		4.6×10^{22}
		^{16}O	5.01×10^{21}		1.0×10^{23}
	:1 part NaCl	^{23}Na	2.58×10^{21}		5.2×10^{22}
Ni	$NiCl_2 \cdot 6H_2O$	^{58}Ni	1.71×10^{21}	16	2.7×10^{22}
Fe	Fe metal	^{56}Fe	9.89×10^{21}	38	3.8×10^{23}
Mg	Mg metal	^{24}Mg	1.95×10^{22}	12	2.3×10^{23}
Cu	Cu metal	^{63}Cu	6.55×10^{21}	7	4.6×10^{22}
		^{65}Cu	2.93×10^{21}		2.1×10^{22}